

See discussions, stats, and author profiles for this publication at: <https://www.researchgate.net/publication/327069500>

Deep Learning for Automated Forgery Detection in Hyperspectral Document Images

Article in *Journal of Electronic Imaging* · September 2018

DOI: 10.1117/1.JEI.27.5.053001

CITATIONS

17

READS

1,706

4 authors:



Muhammad Jaleed Khan

National University of Ireland, Galway

25 PUBLICATIONS 120 CITATIONS

[SEE PROFILE](#)



Adeel Yousaf

11 PUBLICATIONS 108 CITATIONS

[SEE PROFILE](#)



Asad Abbas

Institute of Space Technology

3 PUBLICATIONS 74 CITATIONS

[SEE PROFILE](#)



Khurram Khurshid

Institute of Space Technology

102 PUBLICATIONS 598 CITATIONS

[SEE PROFILE](#)

Some of the authors of this publication are also working on these related projects:



Saliency based visualization of hyperspectral Satellite images [View project](#)



Crowd Management [View project](#)

Deep Learning for Automated Forgery Detection in Hyperspectral Document Images

Muhammad Jaleed Khan,^{a,*} Adeel Yousaf,^b Asad Abbas,^c Khurram Khurshid^a

^aInstitute of Space Technology, Department of Electrical Engineering, Islamabad 44000, Pakistan.

^bInstitute of Space Technology, Department of Aeronautics and Astronautics, Islamabad 44000, Pakistan.

^cThe University of Newcastle, School of Electrical Engineering and Computing, NSW 2308, Australia.

Abstract. Deep learning is revolutionizing the already rapidly developing field of computer vision. Convolutional neural network (CNN) is a state-of-the-art deep learning tool that learns high level features directly from a huge dataset of labelled images. In document image processing, ink analysis allows for determination of ink age and forgery and identification of pen or writer. The spectral information of inks in hyperspectral document images provides valuable information about the underlying material and thus helps in identification and discrimination of inks based on their unique spectral signatures even if they have the same color. Ink mismatch detection is a key step in document forgery detection. Although various ink mismatch detection techniques are available in the recent literature, there is a constant need for development of more accurate and effective methods to empower automated document forgery detection. In this paper, a state-of-the-art deep learning method for ink mismatch detection in hyperspectral document images is proposed. The spectral responses of ink pixels are extracted from a hyperspectral document image, reshaped to a CNN-friendly image format and fed to the CNN for classification. The proposed method effectively identifies different ink types in a hyperspectral document image for forgery detection and achieves an overall accuracy of 98.2% for blue and 88% for black inks, which is the highest accuracy among the latest techniques of ink mismatch detection on the UWA Writing Ink Hyperspectral Images (WIHSI) database¹ and differentiates between the highest number of inks mixed in unbalanced proportions in a hyperspectral document image. Furthermore, a detailed discussion on selection of appropriate CNN architecture and classification results are presented in this paper along with comparison with the former methods of ink mismatch detection. This research opens a new window for research on automated forgery detection in hyperspectral document images using deep learning.

Keywords: Convolutional neural network, deep learning, forgery detection, hyperspectral images, ink mismatch detection.

*Corresponding Author, E-mail: mjk093@gmail.com

1 Introduction

Over the past decade, deep learning has added a huge boost to the field of computer vision. It has shown outstanding performance in the modern computer vision applications ranging from image search, face recognition and photo stylization to drones and self-driving cars. Convolutional neural network (CNN) is a state-of-the-art deep learning tool that extracts spatial features from images using local connections and reduces the dimensionality using reduced connections and shared weights. The complimentary properties of CNN include its invariance to scale, shift, distortion and small rotation². Furthermore, the availability of pre-trained networks and large datasets of labelled data, and the advent of graphical processing units (GPUs) encourage the use of CNN for feature

extraction and image classification tasks. CNN was employed for classification of 1.2 million high-resolution images by Krizhevsky et al.³ in the ImageNet Large Scale Visual Recognition Challenge (LSVRC). CNN has effectively improved feature extraction and image classification systems in a broad range of applications, such as military target detection⁴, speech recognition⁵, natural language processing⁶, character recognition⁷, gaming⁸, breast cancer detection⁹ and large-scale video classification¹⁰. CNN has evolved as an effective tool for classification of hyperspectral images as well¹¹. Sparse representation of deep features extracted by CNN can be used for classification of hyperspectral data¹². Pixel level classification is a common approach in hyperspectral image analysis¹³.

Hyperspectral images (HSIs) provide broad spectral information that allows for identification of the underlying material in images using signal-processing techniques¹⁴. HSI analysis has gained enormous interest in forensic science as it adds to the potential to forensic experts for viewing and interpreting various forensic traces such as fingerprints, inks, bloodstains, hair, drugs etc. The speed and portability of hyperspectral sensing systems has increased tremendously over the last few decades, thus making it the appropriate choice for investigation of forensic traces at crime scenes. Being a non-destructive tool, HSI analysis has been widely used in document imaging for improving readability and determination of ink age, backdating and forgery in documents¹⁵, recovery of erased and overwritten scripts¹⁶ and identification of inks and pigments for dating of manuscripts¹⁷.

Ink mismatch indicates the possibility of forgery in a document. Inks in a potentially fraudulent document are analyzed by forensic specialists and if more than one kind of inks are found in the document, it portrays the possibility of some manipulations made in that document. Various automated ink mismatch detection methods based on HSI are proposed in the recent years. Z. Khan

et al.¹ introduced the idea of ink mismatch detection using HSI and used k-means clustering to differentiate between two different types of ink used in a document. M.J. Khan et al.¹⁸ employed Fuzzy C-Means clustering (FCM) for ink discrimination in hyperspectral document images with several inks mixed in different ratios and achieved much better results after incorporating feature selection. A localized HSI technique was used to leverage the minute differences between quality of inks in original and fake document images by¹⁹. A. Abbas et al.²⁰ proposed a hyperspectral unmixing based ink analysis technique, which was able to distinguish between multiple inks present in a document in unbalanced proportions.

In this paper, we propose a novel technique for ink mismatch detection using HSI analysis and deep learning. Ink pixels are segmented using local thresholding and fed to a CNN for training. The trained CNN is then used to classify ink pixels in a hyperspectral document image based on their spectral responses. The publicly available UWA Writing Ink Hyperspectral Images (WIHSI) database¹ is used for experimentation. A number of samples of inks from different brands are mixed in various proportions to generate mixed ink combinations for experiments. Contributions of this paper are listed below:

1. A CNN based novel method for ink mismatch detection in hyperspectral images is proposed which detects ink mismatch by classifying the ink pixels based on their spectral responses.
2. The optimum architecture of CNN for this purpose is determined by experimenting six different architectures with different number of layers with different filter sizes in the convolutional layers. The optimum architecture contains four convolutional layers each with a filter size of 3x3 is determined

3. The proposed method achieved the highest accuracy (98.2% for blue inks and 88% for black inks) on the UWA WIHSI database ¹ among the former methods of ink mismatch detection in hyperspectral images with multiple inks mixed in unbalanced proportions.
4. The CNN trained with blue inks also achieves an accuracy of 85% on black inks, which shows that CNN learns generic features from the dataset.

The rest of the paper is organized as follows: Related work is reviewed in Section II, the proposed method is explained in detail in Section III, the experimental results are presented in Section IV and Section V concludes the paper.

2 Related Work

Hyperspectral image analysis has significantly improved the efficiency of forgery detection systems over the recent years. Various HSI based techniques for automated forgery detection are proposed in literature. E.B. Brauns et al. ²¹ developed a hyperspectral sensing system for non-destructive forgery detection in questioned documents by employing an interferometer. Different moving parts were used for frequency tuning and subsequently moderating or slowing down the acquisition procedure. Subjective outcomes on a small database demonstrated that the proposed unsupervised learning based technique effectively discriminated different inks based on the ink spectra. The results of this research endorses and encourages the use of HSI analysis for discrimination between different inks in a questioned document. A comparatively complex and advanced hyperspectral imaging framework for historic document examination was developed at the National Archives of Netherlands that provided high resolution in the spatial as well as the spectral domain, i.e. ranging from near ultraviolet to near infrared²². Though the system was very robust and efficient for analysis of ancient documents but the acquisition time of hyperspectral

sensors was very long²³. Ink-deposition traces²⁴ and texture²⁵ have been used for writing analysis in document images in the past.

HSI bears a tremendous potential for accurate differentiation of materials based on their unique spectral signatures²⁶. Even the spectrum of a single pixel in HSI can provide extensively rich information content about the surface of the material as compared to color image. R.J. Hejdam et al.²⁷ used HSI analysis for refurbishment of ancient documents, and targeted the practical scenarios where ink could not be detected by naked eyes. F. Hollaus et al.²⁸ proposed image enhancement for degraded images by utilizing the spectral as well as spatial information. C.S. Silva et al.²⁹ employed chemometrics and used the age information of various inks to detect forgery in questioned documents using HSI analysis. A. Morales et al.³⁰ employed HSI analysis and least square SVM classification for ink analysis in an embedded system. A forgery detection system based on HSI analysis is proposed by Z. Khan et al.¹ that employs k-means clustering after optimum bands selection for discrimination of different inks in a potentially fake document. However, an assumption for experimentation has been made that the text in document is composed for two types of inks in equal proportion, due to which this method may not be applicable in practical situations where small manipulations are made in the document. Z. Luo et al.¹⁹ proposed forgery detection in documents based on localized HSI analysis, by leveraging the visually negligible differences between the quality of inks in forged and original documents. A. Abbas et al.²⁰ proposed a novel unsupervised clustering method for distinguishing between inks from various brands in varying mixing ratios in a document based on hyperspectral unmixing. However, this accuracy reduces in this method as the number of mixed inks increase and mixing ratio of the inks vary in unbalanced proportion. An ink mismatch detection system, that is robust against

varying mixing ratios of inks and increased number of inks in a document, is required for its implementation for practical use.

It is a common practice in HSI analysis to classify each pixel independently¹³. Due to spatial variability of spectral responses, feature extraction is a challenging task in HSI analysis³¹. The linear transform methods such as Principal Component Analysis (PCA), Independent Component Analysis (ICA) and Linear Discriminant Analysis (LDA), kernel based methods such as Hilbert technique and manifold learning and single layer methods have been widely used for feature extraction and classification but their performance is not up to the mark in image classification tasks. However, multilayer systems work very well in image classification tasks³². The modern deep learning techniques extract new features from data using two or more layers that results in high performance in image classification tasks³. Stacked autoencoders with sparse representation of features is proposed for HSI classification in³³. Y. Chen et al.³⁴ proposed spatial-spectral hybrid features for image classification using deep belief network (DBN). Aforementioned deep learning techniques include many training parameters due to full connection between layers, which is undesirable in case of limited training data.

Convolutional Neural Network (CNN) is a state-of-the-art deep learning tool that is well suited for image recognition tasks. Representative features are efficiently extracted from images using local connections, which can result in high dimensionality. Reduced connections and shared weights are used to reduce the curse of dimensionality. The architecture of CNN comprises several alternating convolutional layers, activation layers and pooling layers. The convolutional layers, which are based on convolutional kernels and local receptive fields, perform 2D convolutions that extract representative features and activations irrespective of their spatial locations in the image, thus making CNN invariant to shift, rotation and scale³. The pooling layers reduce the learning

parameters in the following layer. A. Romero et al.³⁵ used CNN for analysis of remote sensing images in an unsupervised greedy manner. Supervised CNN leverages the class specific information in the training data to extract optimum features³⁶. CNN has the capability to learn optimum features from the spectral response of a pixel. The spectral responses can be reshaped into 2D form and directly fed to the CNN. The high dimensionality of hyperspectral images is minimized by weight sharing and reduction of train parameters in CNN. Furthermore, over-fitting caused by limited training samples of HSIs is minimized by using several regularization methods, which can use dropout and rectified linear unit (ReLU) to generalize the CNN³⁶.

3 Proposed Document Forgery Detection System

3.1 Database and Preprocessing

The UWA Writing Inks Hyperspectral Images (WIHSI) database¹ contains 14 hyperspectral data cubes, each with 33 channels in the visible spectral range of 480~720nm. A single document contains five English phrases written by one of the seven authors with five different inks of either blue or black color. The example of a single document is shown in Figure 2(a). Each ink came from different manufacturer to ensure subtle variations within the inks of the same color as shown in Figure 1.



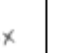
RGB	460nm	520nm	580nm	640nm	700nm
					
					

Fig. 1. Segmented ink pixels in the selected spectral bands of an HSI for two different blue inks demonstrating the ink discrimination offered by hyperspectral imaging.

Due to the non-uniform illumination over the images, Sauvola's local thresholding³⁷ is employed to compute binary masks representing ink pixels in the hyperspectral images as shown in Figure

2(b). Each hyperspectral image is decomposed into five hyperspectral images, as shown in Figure 2(c), each containing one line of the English phrase written with a single ink type.

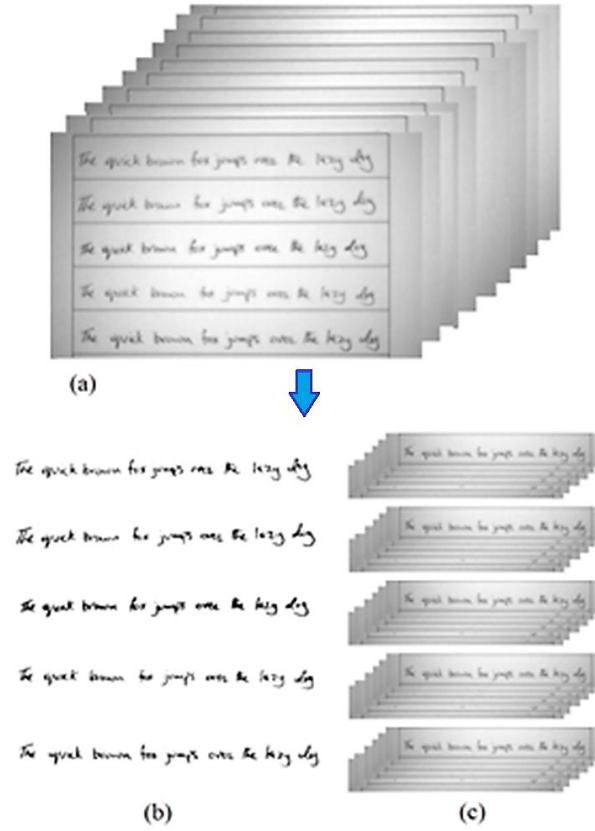


Fig. 2. (a) HSI with 33 bands, (b) binary masks for segmentation of text, and (c) decomposition into five hyperspectral images each with a single phrase.

3.2 Hyperspectral Mixing of Ink Samples

In order to analyze the performance of the proposed method for different scenarios, mixed combinations of different inks are generated by merging image portions in different proportion from two different ink samples of the same color and written by the same author. This process of mixing ink samples is illustrated by an example in Figure 3. No black and blue ink samples were mixed with each other because such mixture of inks can be easily distinguished by visual examination. The mixed ink combinations are summarized in Table 1. These images are used as

ground truth images during experimentation to assess the performance of the proposed method as shown in Figure 8. For better visualization, each ink is represented by a different color.

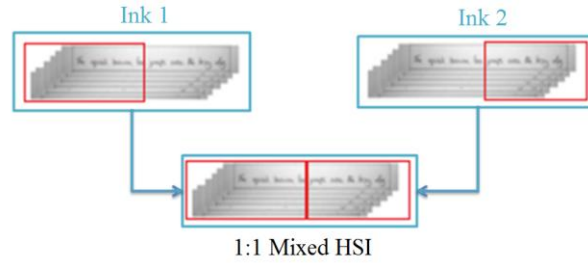


Fig. 3. An example of hyperspectral mixing: two different ink samples of the same color are merged in equal proportion.

Table 1. Mixed ink combinations with different number of inks of the same color mixed in different proportions

Combination	No. of Inks Mixed	Mixing Ratio
A	2	1:1
B	2	1:4
C	2	1:8
D	2	1:16
E	2	1:32
F	3	1:1:1
G	4	1:1:1:1
H	5	1:1:1:1:1

3.3 Spectral Data Organization

In order to classify an ink pixel based on its spectral response, we need to format the spectral responses in image form because CNN is well suited for image data. The spectral response of a pixel is a 1x33 vector, which is reshaped to 6x6 matrix with three zeros at the end, as illustrated in Figure 4.

3.4 CNN Architectures and Training Process

Several factors determine the architecture of CNN for any application. We designed different CNN architectures with different number of layers, and each convolutional layer comprising of different number of filters and different filter sizes. We have experimented two different filter sizes, i.e. 3x3 to 5x5 in our CNN architectures. With each filter size, three different sets of convolutional layers

are used, i.e. 2, 4 and 6 convolutional layers with alternating ReLU and pooling layers and varying number of filters. The six different CNN architectures as presented in detail in Table 2. The parameters of each layer i.e. filter size and/or number of filters are mentioned with each layer in parenthesis. A dropout layer is used to minimize over-fitting further. The final layer contains five neurons representing five ink types. The dataset ¹ comprises five distinct ink types of blue and black colors. We can easily distinguish between blue and black inks by visual inspection or using color image processing; therefore, color-based classification is not dealt in the hyperspectral analysis based approach. Each CNN architecture is separately trained and tested for blue and black inks. Later on, it was noticed that CNN extracts generic features and the CNN trained with blue inks works very well on black inks as well.

Table 2. Details and comparison of different CNN architectures

CNN - 1	CNN - 2	CNN - 3	CNN - 4	CNN - 5	CNN - 6
<i>Network Layers</i>					
InputLayer	InputLayer	InputLayer	InputLayer	InputLayer	InputLayer
ConvLayer1(3x3, 6)	ConvLayer1(5x5, 6)	ConvLayer1(3x3, 6)	ConvLayer1(5x5, 6)	ConvLayer1(3x3, 6)	ConvLayer1(5x5, 6)
ReLU-Layer	ReLU-Layer	ReLU-Layer	ReLU-Layer	ReLU-Layer	ReLU-Layer
ConvLayer2(3x3, 18)	ConvLayer2(5x5, 18)	ConvLayer2(3x3, 18)	ConvLayer2(5x5, 18)	ConvLayer2(3x3, 18)	ConvLayer2(5x5, 18)
ReLU-Layer	ReLU-Layer	ReLU-Layer	ReLU-Layer	ReLU-Layer	ReLU-Layer
MaxPooling1(2x2)	MaxPooling1(2x2)	MaxPooling1(2x2)	MaxPooling1(2x2)	MaxPooling1(2x2)	MaxPooling1(2x2)
Dropout-Layer	Dropout-Layer	ConvLayer3(3x3, 36)	ConvLayer3(5x5, 6)	ConvLayer3(3x3, 36)	ConvLayer3(5x5, 6)
Fully-Connected(5)	Fully-Connected(5)	ReLU-Layer	ReLU-Layer	ReLU-Layer	ReLU-Layer
Softmax-Layer	Softmax-Layer	ConvLayer4(3x3, 54)	ConvLayer4(5x5, 18)	ConvLayer4(3x3, 54)	ConvLayer4(5x5, 18)
		ReLU-Layer	ReLU-Layer	ReLU-Layer	ReLU-Layer
		MaxPooling2(2x2)	MaxPooling2(2x2)	MaxPooling2(2x2)	MaxPooling2(2x2)
		Dropout-Layer	Dropout-Layer	ConvLayer5(3x3, 72)	ConvLayer5(5x5, 72)
		Fully-Connected(5)	Fully-Connected(5)	ReLU-Layer	ReLU-Layer
		Softmax-Layer	Softmax-Layer	ConvLayer6(3x3, 90)	ConvLayer6(5x5, 90)
				ReLU-Layer	ReLU-Layer
				MaxPooling3(2x2)	MaxPooling3(2x2)
				Dropout-Layer	Dropout-Layer
				Fully-Connected(5)	Fully-Connected(5)
				Softmax-Layer	Softmax-Layer
<i>Number of Train Parameters</i>					
2,346	4,188	37,500	80,796	163,464	372,648
<i>Average Accuracy (Blue, Black)</i>					
(96.8, 85.1)	(95.4, 85)	(98.2, 88)	(97.1, 86.2)	(65.6, 60.3)	(59.8, 51.8)

For training the CNN, spectral responses are extracted from all hyperspectral images corresponding to six out of seven authors in the dataset ¹ and stored along with their respective labels of each ink type. The spectral responses of ink pixels of text one author are used to test the

CNN. The total number of spectral responses collected from the dataset ¹ are summarized in Table 3. Selection of appropriate architecture and training parameters aids CNN in learning optimum features from the dataset. The training parameters set for each CNN are listed in Table 4.

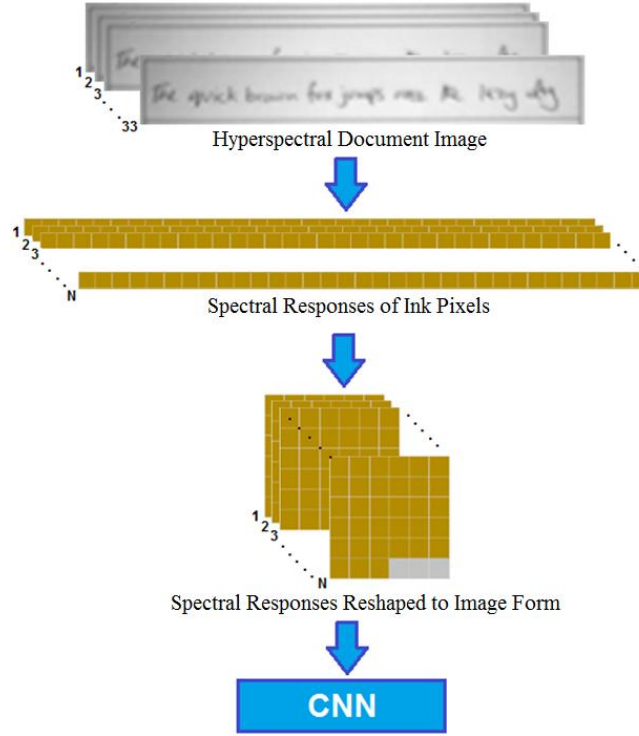


Fig. 4. Strategy adopted for classification of the ink pixels based on their spectral responses using CNN.

3.5 CNN Classification for Ink Mismatch Detection

The trained CNN is used for classifying ink pixels to detect ink mismatch in an input hyperspectral image of a questioned document after the preprocessing steps. The spectral response of each ink pixel is extracted, reshaped and passed to the CNN for classification. After classification, the ink pixels in the hyperspectral image are labelled for the sake of visualization of any potential ink mismatch in the document. Examples of each mixed ink combination are shown in Figure 8.

Table 3. Statistics of spectral responses for training and testing the CNN

Ink Color	No. of Ink Types	No. of spectral response samples		
		Training (6 Authors)	Testing (1 Author)	Total (7 Authors)
Black	5	94,984	14,718	109,702
Blue	5	97,148	15,420	112,568
Total	10	192,132	30,138	222,270

Table 4. CNN Training Parameters

Parameter	Value
Mini Batch Size	500
Max Epochs	15
Initial Learn Rate	0.05
Learn Rate Drop Factor	0.2
Learn Rate Drop Period	5
Optimizer	SGDM
Momentum	0.9

4 Experimental Results

MATLAB R2017a was used for all experiments on a workstation with 64GB RAM, Intel 2.3 GHz, 64-bit processor with 18 cores. NVIDIA GPU with 12GB memory and compute capability of 3.5 was used for training the CNNs. The six CNN architectures were trained with the spectral responses of blue and black inks collected from the dataset ¹. The spectral responses of ink pixels of the text written by six authors were used for training while that of one author were used for testing as shown in Table 3. Accuracy is defined as the number of correctly labeled pixels divided by the total number of pixels in the image ¹. The accuracy achieved by each CNN architecture for both blue and black inks is presented in Figure 5(b). Promising results were noted during this analysis. Due to the small input image size i.e. 6x6 pixels, the CNN architectures with the smallest filter size of 3x3 achieved highest accuracy as compared to the filter size of 5x5. It was observed

that using lower number of filters in initial layers and increasing the number of layers in the deeper layers resulted in higher accuracy.

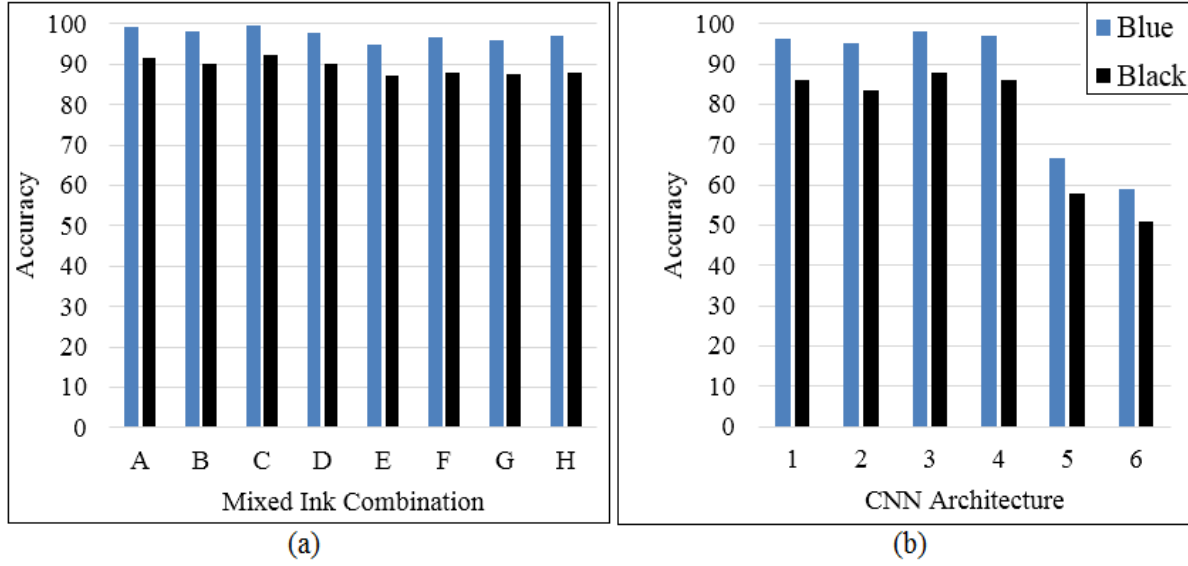


Fig. 5. (a) Test accuracy achieved by the trained CNN-3 on each mixed ink combination. (b) Accuracy achieved by each CNN architecture with different number of layers and different convolution filter size.

Among the six CNN architectures, CNN-3 achieved the highest accuracy of 98.2% for blue inks and 88% for black inks. This shows that the CNN Architecture-3 with four convolutional layers with number of filters increasing in each following convolutional layer is the optimum architecture for the proposed approach. Block diagram of the optimal architecture, CNN-3 is presented in Figure 6. After these observations, CNN-3 was used for further experiments. The training accuracy plots and training loss plots for all CNN architectures are shown in Figure 7(a) and Figure 7(b) respectively. CNN-3 starts converging after approximately 400 iterations but converges quickly to the minimum error among the other CNN architectures. It was also noted that the CNN learns generic features from the training dataset of spectral responses and the CNN trained with blue inks achieves a testing accuracy of 85% on black inks. Training time for CNN-3 was 240 seconds and each input hyperspectral image took 13.4 seconds for all processing steps including classification

using CNN-3. The CNN Architecture-3 was tested on the mixed ink combinations presented in Table 1. The accuracies obtained by the CNN on each mixed ink combinations of both blue and black inks are presented in Figure 5(a).

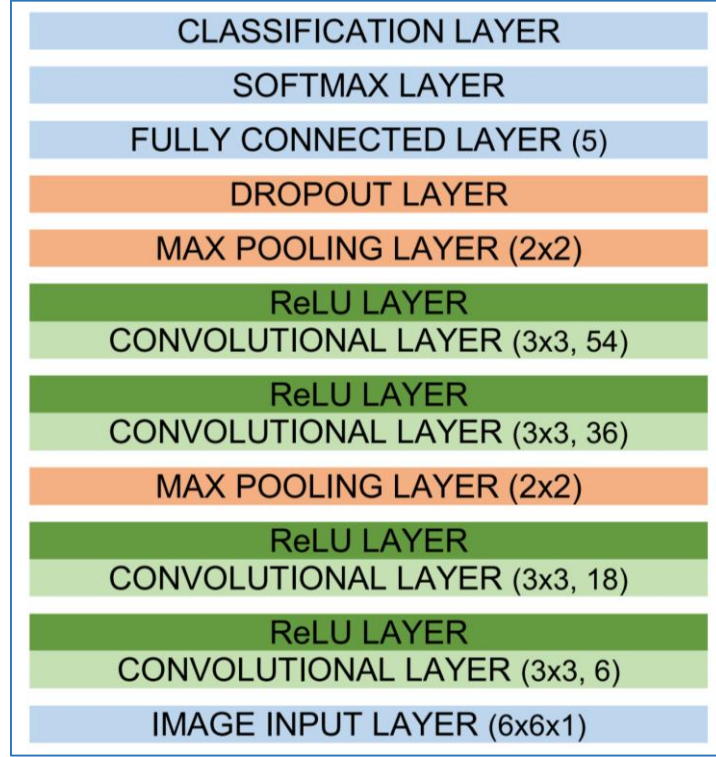


Fig. 6. Block diagram of the optimal architecture CNN-3

CNN usually gives better performance with smaller filters because larger filters can overlook some features and skip the essential details in the images. The input image size in the proposed system is very small, i.e. 6x6, for which only a smaller filter size can be used. Therefore only small filters with sizes 3x3 and 5x5 were experimented. It is observed that the architectures with filters of size 3x3 achieve better accuracy than the same architecture with filters of size 5x5, e.g. CNN-3 with filter size 3x3 achieves better accuracy as compared to CNN-4 with the same layers and filter size of 5x5.

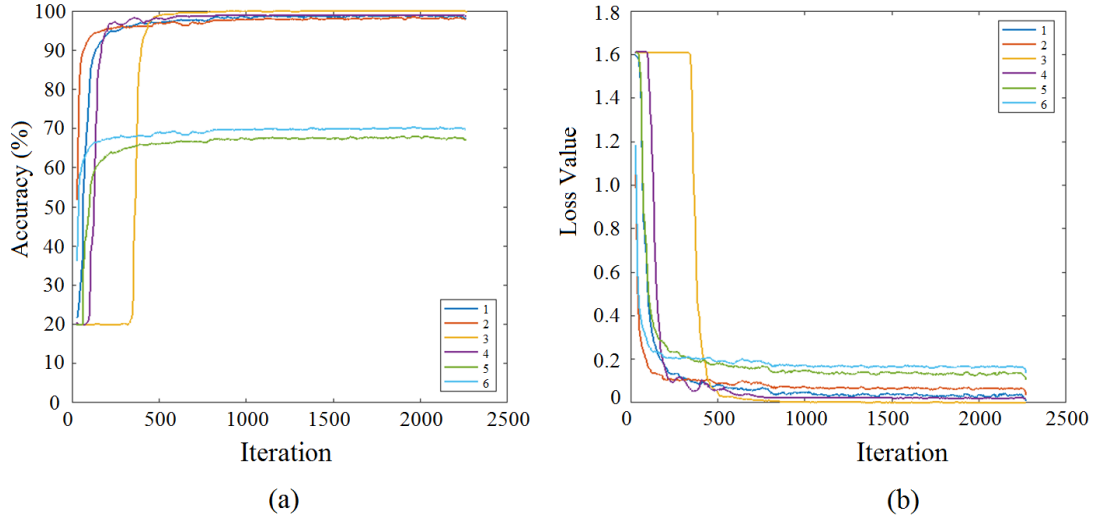


Fig. 7. (a) Training accuracy plots, and (b) training loss plots of all CNN architectures.

An average accuracy of 98.2% and 88% was noted for blue and black inks respectively. This is the highest accuracy attained so far in ink mismatch detection on the UWA WIHSI dataset. The qualitative comparisons of the ground truth images and the final segmentation results are presented in Figure 8. It can be seen that all ink pixels are correctly classified except a few misclassifications in the results of Combination G and H. A detailed comparison with the previous methods on this subject ^{1,19,20} on the same dataset is summarized in Table 5, which shows that the proposed method outclasses previous methods on this subject by achieving the highest accuracy and correctly discriminating between the highest number of inks mixed in unbalanced proportions. Moreover, CNN employed in the proposed system is invariant to scale, shift and rotation. Thus, the proposed method is robust against such transformations. However, the proposed system is applicable in scenarios where information about the inks used in a questioned document is available as a priori due to usage of supervised classification. Unsupervised deep learning can help in eliminating the requirement of prior knowledge of data and trained classifier for quick investigation of questioned documents.

Combo	Type	Image
A (Ink1~2)	Ground Truth	
	Final Result	
B (Ink1~2)	Ground Truth	
	Final Result	
C (Ink1~2)	Ground Truth	
	Final Result	
D (Ink1~2)	Ground Truth	
	Final Result	
E (Ink1~2)	Ground Truth	
	Final Result	
F (Ink1~3)	Ground Truth	
	Final Result	
G (Ink1~4)	Ground Truth	
	Final Result	
H (Ink1~5)	Ground Truth	
	Final Result	

Fig. 8. Comparison of segmentation results and ground truth images of hyperspectral document images with mixed inks.

Table 5. Comparison of results obtained by the proposed method with the previous methods

Method	Average Accuracy (%)	Number of inks mixed	Unbalanced ink proportions
Proposed Approach	98.2 (Blue) 88 (Black)	2~5	Yes
A. Abbas et al. ²⁰	86.2 (Blue) 83.4 (Black)	2~4	Yes
Z. Luo et al. ¹⁹	89.0 (Blue) 82.3 (Black)	2	Yes
Z. Khan et al. ¹	85.6 (Blue) 81.4 (Black)	2	No

5 Conclusion and Future Prospects

Hyperspectral image analysis of questioned documents provides valuable information about the underlying material and thus allows for distinguishing between visually similar inks. Ink mismatch in a questioned document indicates forgery. Deep learning has added a boost to many computer vision applications in the recent years. Convolutional Neural Network (CNN) is being widely used in image recognition tasks. In this paper, a novel method for ink mismatch detection in hyperspectral document images using CNN is proposed. Spectral responses of ink pixels are extracted from the hyperspectral images using Sauvola’s local thresholding, reshaped to image form and classified using CNN. The proposed method effectively identifies different ink types in a hyperspectral document image for forgery detection and achieves an overall accuracy of 98.2% for blue inks and 88% for black inks on the UWA WIHSI database, which is the highest accuracy among the former methods of ink mismatch detection in hyperspectral images with highest number of inks mixed in unbalanced proportions. This work opens a new window for research in document forgery detection using deep learning and hyperspectral image analysis. However, the applicability of the proposed system is limited to scenarios where information about the inks used in a questioned document is available a priori due to usage of supervised classification. In the future work, we plan to incorporate both spectral and spatial features for classification of a target pixel by also considering its neighboring pixels. We will also explore unsupervised deep learning for

automated forgery detection to eliminate the requirement of prior knowledge of data and trained classifier for quick investigation of questioned documents.

References

1. Z. Khan, F. Shafait, and A. Mian, "Hyperspectral Imaging for Ink Mismatch Detection," in 2013 12th International Conference on Document Analysis and Recognition, pp. 877–881, IEEE (2013) [doi:10.1109/ICDAR.2013.179].
2. Y. Lecun et al., "Gradient-based learning applied to document recognition," Proc. IEEE **86**(11), 2278–2324 (1998) [doi:10.1109/5.726791].
3. A. Krizhevsky, I. Sutskever, and G. E. Hinton, "ImageNet Classification with Deep Convolutional Neural Networks," pp. 1097–1105 (2012).
4. M. J. Khan et al., "Automatic Target Detection in Satellite Images using Deep Learning," J. Sp. Technol. **7**(1), 44–49 (2017).
5. T. N. Sainath et al., "Deep Convolutional Neural Networks for Large-scale Speech Tasks," Neural Networks **64**, 39–48, Pergamon (2015) [doi:10.1016/J.NEUNET.2014.08.005].
6. Y. Kim, "Convolutional Neural Networks for Sentence Classification" (2014).
7. A. Yousaf et al., "Benchmark dataset for offline handwritten character recognition," in 2017 13th International Conference on Emerging Technologies (ICET) (2017) [doi:10.1109/ICET.2017.8281752].
8. D. Silver et al., "Mastering the game of Go with deep neural networks and tree search," Nature **529**(7587), 484–489, Nature Publishing Group (2016) [doi:10.1038/nature16961].
9. S. Charan, M. J. Khan, and K. Khurshid, "Breast cancer detection in mammograms using convolutional neural network," in 2018 International Conference on Computing, Mathematics and Engineering Technologies (iCoMET), pp. 1–5, IEEE (2018) [doi:10.1109/ICOMET.2018.8346384].
10. Karpathy A, Toderici G, and Shetty S, "Large-scale video classification with convolutional neural

- networks,” in Proceedings of the IEEE conference on Computer Vision and Pattern Recognition, pp. 1725–1732 (2014).
11. Y. Chen et al., “Deep Learning-Based Classification of Hyperspectral Data,” *IEEE J. Sel. Top. Appl. Earth Obs. Remote Sens.* **7**(6), 2094–2107 (2014) [doi:10.1109/JSTARS.2014.2329330].
 12. H. Liang and Q. Li, “Hyperspectral Imagery Classification Using Sparse Representations of Convolutional Neural Network Features,” *Remote Sens.* **8**(2), 99, Multidisciplinary Digital Publishing Institute (2016) [doi:10.3390/rs8020099].
 13. J. M. Bioucas-Dias et al., “Hyperspectral Remote Sensing Data Analysis and Future Challenges,” *IEEE Geosci. Remote Sens. Mag.* **1**(2), 6–36 (2013) [doi:10.1109/MGRS.2013.2244672].
 14. M. J. Khan et al., “Modern Trends in Hyperspectral Image Analysis: A Review,” *IEEE Access* **6**(1), 14118–14129 (2018) [doi:10.1109/ACCESS.2018.2812999].
 15. S. Joo Kim, F. Deng, and M. S. Brown, “Visual enhancement of old documents with hyperspectral imaging,” *Pattern Recognit.* **44**(7), 1461–1469, Pergamon (2011) [doi:10.1016/J.PATCOG.2010.12.019].
 16. C. Balas et al., “A novel hyper-spectral imaging apparatus for the non-destructive analysis of objects of artistic and historic value,” *J. Cult. Herit.* **4**, 330–337, Elsevier Masson (2003) [doi:10.1016/S1296-2074(02)01216-5].
 17. K. Melessanaki et al., “Laser induced breakdown spectroscopy and hyper-spectral imaging analysis of pigments on an illuminated manuscript,” *Spectrochim. Acta Part B At. Spectrosc.* **56**(12), 2337–2346, Elsevier (2001) [doi:10.1016/S0584-8547(01)00302-0].
 18. M. J. Khan et al., “Automated Forgery Detection in Multispectral Document Images using Fuzzy Clustering,” in 13th IAPR International Workshop on Document Analysis Systems, IEEE, Vienna, Austria (2018) [doi:10.1109/DAS.2018.26].
 19. Z. Luo, F. Shafait, and A. Mian, “Localized forgery detection in hyperspectral document images,” in 2015 13th International Conference on Document Analysis and Recognition (ICDAR), pp. 496–500, IEEE (2015) [doi:10.1109/ICDAR.2015.7333811].

20. A. Abbas, K. Khurshid, and F. Shafait, "Towards Automated Ink Mismatch Detection in Hyperspectral Document Images," in 2017 14th IAPR International Conference on Document Analysis and Recognition (ICDAR), pp. 1229–1236, IEEE (2017) [doi:10.1109/ICDAR.2017.203].
21. E. B. Brauns and R. B. Dyer, "Fourier Transform Hyperspectral Visible Imaging and the Nondestructive Analysis of Potentially Fraudulent Documents," *Appl. Spectrosc.* **60**(8), 833–840, Society for Applied Spectroscopy (2006).
22. R. Padoan et al., "Quantitative hyperspectral imaging of historical documents: technique and applications," in ART Proceedings (2008).
23. M. Klein et al., "Quantitative Hyperspectral Reflectance Imaging," *Sensors* **8**(9), 5576–5618, Molecular Diversity Preservation International (2008) [doi:10.3390/s8095576].
24. K. Franke and S. Rose, "Ink-Deposition Model: The Relation of Writing and Ink Deposition Processes," in Ninth International Workshop on Frontiers in Handwriting Recognition, pp. 173–178, IEEE [doi:10.1109/IWFHR.2004.59].
25. K. Franke, O. Bunne Meyer, and T. Sy, "Ink texture analysis for writer identification," in Proceedings Eighth International Workshop on Frontiers in Handwriting Recognition, pp. 268–273, IEEE Comput. Soc (2002) [doi:10.1109/IWFHR.2002.1030921].
26. D. Landgrebe, "Information Extraction Principles and methods for multispectral and hyperspectral image data," in Information Processing For Remote Sensing, pp. 3–37, World Scientific (1999) [doi:10.1142/9789812815705_0001].
27. R. Hedjam, M. Cheriet, and M. Kalacska, "Constrained Energy Maximization and Self-Referencing Method for Invisible Ink Detection from Multispectral Historical Document Images," in 2014 22nd International Conference on Pattern Recognition, pp. 3026–3031, IEEE (2014) [doi:10.1109/ICPR.2014.522].
28. F. Hollaus, M. Gau, and R. Sablatnig, "Enhancement of Multispectral Images of Degraded Documents by Employing Spatial Information," in 2013 12th International Conference on

- Document Analysis and Recognition, pp. 145–149, IEEE (2013) [doi:10.1109/ICDAR.2013.36].
29. C. S. Silva et al., “Near infrared hyperspectral imaging for forensic analysis of document forgery,” *Analyst* **139**(20), 5176–5184, The Royal Society of Chemistry (2014) [doi:10.1039/C4AN00961D].
 30. A. Morales et al., “The use of hyperspectral analysis for ink identification in handwritten documents,” in 2014 International Carnahan Conference on Security Technology (ICCST), pp. 1–5, IEEE (2014) [doi:10.1109/CCST.2014.6986980].
 31. X. Jia, B.-C. Kuo, and M. M. Crawford, “Feature Mining for Hyperspectral Image Classification,” *Proc. IEEE* **101**(3), 676–697 (2013) [doi:10.1109/JPROC.2012.2229082].
 32. N. Kruger et al., “Deep Hierarchies in the Primate Visual Cortex: What Can We Learn for Computer Vision?,” *IEEE Trans. Pattern Anal. Mach. Intell.* **35**(8), 1847–1871 (2013) [doi:10.1109/TPAMI.2012.272].
 33. Chao Tao et al., “Unsupervised Spectral–Spatial Feature Learning With Stacked Sparse Autoencoder for Hyperspectral Imagery Classification,” *IEEE Geosci. Remote Sens. Lett.* **12**(12), 2438–2442 (2015) [doi:10.1109/LGRS.2015.2482520].
 34. Y. Chen, X. Zhao, and X. Jia, “Spectral–Spatial Classification of Hyperspectral Data Based on Deep Belief Network,” *IEEE J. Sel. Top. Appl. Earth Obs. Remote Sens.* **8**(6), 2381–2392 (2015) [doi:10.1109/JSTARS.2015.2388577].
 35. A. Romero, C. Gatta, and G. Camps-Valls, “Unsupervised Deep Feature Extraction for Remote Sensing Image Classification,” *IEEE Trans. Geosci. Remote Sens.* **54**(3), 1349–1362 (2016) [doi:10.1109/TGRS.2015.2478379].
 36. Y. Chen et al., “Deep Feature Extraction and Classification of Hyperspectral Images Based on Convolutional Neural Networks,” *IEEE Trans. Geosci. Remote Sens.* **54**(10), 6232–6251 (2016) [doi:10.1109/TGRS.2016.2584107].
 37. F. Shafait, D. Keysers, and T. M. Breuel, “Efficient implementation of local adaptive thresholding techniques using integral images,” in *Document Recognition and Retrieval XV* **6815**, B. A.

Yanikoglu and K. Berkner, Eds., pp. 681510-681510–681516, International Society for Optics and Photonics, San Jose, CA, USA (2008) [doi:10.1117/12.767755].

First Author is a postgraduate student in Institute of Space Technology, Pakistan. He received his BS degree in the field of Computer Engineering from University of Engineering & Technology, Peshawar, Pakistan in 2015 and MS degree in Electrical Engineering with specialization in Signal & Image Processing from Institute of Space Technology, Islamabad, Pakistan in 2017. His research interests are computer vision, hyperspectral image analysis and deep learning.

Second Author is a research associate in Institute of Space Technology, Pakistan. He received his BS degree in the field of Electrical Engineering from University of Engineering & Technology, Taxila, Pakistan and MS degree in Electrical Engineering with specialization in Signal & Image Processing from Institute of Space Technology, Pakistan in 2017. His research interests include computer vision, machine learning and genetic programming.

Third Author is a PhD student in University of Newcastle, Australia. He received his BSc. degree in field of Electrical Engineering from University of Engineering and Technology, Taxila, Pakistan in 2012 and Master's degree in Electrical Engineering with Specialization in Signal and Image Processing from Institute of Space Technology, Islamabad in 2015. His research interests include pattern recognition, computer vision and deep learning.

Fourth Author is working as Associate Professor at the Department of Electrical Engineering and head of the Signal & Image Processing research group at Institute of Space Technology, Pakistan. He received his PhD in Computer Vision from Paris Descartes University, Paris, France in 2009. He is the pioneer of Pakistani Pattern Recognition Society which is an official branch of IAPR in Pakistan. He is the editor of Journal of Space Technology and the project director of IST's CubeSat

program. His research interests include hyperspectral image analysis, computer vision and small satellite design and development.

List of Figure Captions

Figure 1	Segmented ink pixels in the selected spectral bands of an HSI for two different blue inks demonstrating the ink discrimination offered by hyperspectral imaging.
Figure 2	(a) HSI with 33 bands, (b) binary masks for segmentation of text, and (c) decomposition into five hyperspectral images each with a single phrase.
Figure 3	An example of hyperspectral mixing: two different ink samples of the same color are merged in equal proportion.
Figure 4	Strategy adopted for classification of the ink pixels based on their spectral responses using CNN
Figure 5	(a) Test accuracy achieved by the trained CNN-3 on each mixed ink combination. (b) Accuracy achieved by each CNN architecture with different number of layers and different convolution filter size.
Figure 6	Block diagram of the optimal architecture CNN-3
Figure 7	(a) Training accuracy plots, and (b) training loss plots of all CNN architectures.
Figure 8	Comparison of segmentation results and ground truth images of hyperspectral document images with mixed inks.